Accepted Manuscript

The effect of the composting time on the gaseous emissions and the compost stability in a full-scale sewage sludge composting plant

Daniel González, Joan Colón, David Gabriel, Antoni Sánchez

Please cite this article as: Daniel González, Joan Colón, David Gabriel, Antoni Sánchez , The effect of the composting time on the gaseous emissions and the compost stability in a full-scale sewage sludge composting plant. Stoten (2018), https://doi.org/10.1016/j.scitotenv.2018.11.081

The effect of the composting time on the gaseous emissions and the compost stability in a full-scale sewage sludge composting plant

Daniel González [a, b], Joan Colón [c], David Gabriel [b], Antoni Sánchez [a,*]

[a] Composting Research Group (GICOM) Dept. of Chemical, Biological and Environmental Engineering, Universitat Autònoma de Barcelona, 08193-Bellaterra (Barcelona), Spain.

[b] Group of biological treatment of liquid and gaseous effluents (GENOCOV) Dept. of Chemical, Biological and Environmental Engineering, Universitat Autònoma de Barcelona, 08193-Bellaterra (Barcelona), Spain

[c] BETA Technology Centre: "U Science Tech", University of Vic-Central University of Catalonia, 08500 Vic, Barcelona, Spain

* Corresponding author:

Antoni Sánchez

Composting Research Group (GICOM), Dept. of Chemical, Biological and Environmental Engineering

Universitat Autònoma de Barcelona

Bellaterra, 08193 (Spain)

Email address: antoni.sanchez@uab.cat

Abstract

Volatile organic compounds (VOCs) and ammonia are some of the compounds present in gaseous emissions from waste treatment facilities that contribute to odour pollution. In the present work, the effect of the residence time on the biological stability of raw sludge (RS) composted in dynamic windrows and the gaseous emissions generated were studied at a full-scale composting plant, aiming to provide specific pollutant emission factors and to determine their variability depending on the composting time. Waste stability and emissions analysis considered both a first phase where mixed RS and vegetal fraction (RS – VF) is actively composted in dynamic windrows and a second standard curing phase in turned piles, which lasted 31 days. Two windrows were operated at 4 days of composting time while two other windrows were operated simultaneously at 14 days composting time. Increasing the residence time lead to a better waste stabilization in the first composting phase, providing a 50% reduction of the Dynamic Respiration Index. A decrease of the ammonia emission factor was achieved when increasing the composting time (from 168.5 g $NH_3 \cdot Mg^{-1}RS – VF \cdot d^{-1}$ to 114.3 g $NH_3 \cdot Mg^{-1}RS – VF \cdot d^{-1}$), whereas the VOCs emission factor was maintained for the same process conditions (between 26.0 and 28.0 g C-VOC$\cdot Mg^{-1}RS – VF \cdot d^{-1}$). However, an increase of the emission masses of both pollutants was observed (from 0.16 to 0.39 kg tVOCs$\cdot Mg^{-1}RS – VF$ and from 1.21 to 1.60 kg $NH_3 \cdot Mg^{-1}RS – VF$). Finally, ammonia and VOCs emissions generated at the curing piles were nearly avoided when increasing the composting time of the first phase.

Keywords: Composting, wastewater sludge, gaseous emissions, VOC, ammonia, biological stability.

1. Introduction

Sewage sludge is generated in large amounts during the whole treatment of wastewater. Its production in European countries totals over 3.5 million Mg per year (dry basis) (Eurostat, 2015). In order to handle and manage this waste, different technologies are applied, such as land application, landfilling, incineration or composting, which is the main biological process applied to sewage sludge in Europe, used to treat about the 14% of its European production (Colón et al., 2017). Sludge is rich in organic matter, nitrogen, phosphorus and other microelements, which makes it a useful raw material to be composted. In addition to these elements, sludge can also contain toxic compounds such as heavy metals or organic pollutants and pathogenic organisms (Kosobucki et al., 2000).

Sewage sludge composting is regarded as an environmental friendly technology that can effectively decompose organic matter into a stable end product. Moreover, the high temperature reached due to the metabolic heat generated during the thermophilic phase of the composting process is effective in destroying pathogens and enhance biological degradation of different organic micro-pollutants (Sadef et al., 2014), allowing the final product to be safely used as fertiliser or soil conditioner (Sánchez et al., 2015). The Working Document on Sludge and Biowaste (European Commission, 2010) sets different combinations of temperature and time in order to reach a proper disinfection of the final product, ranging from temperatures over 55ºC and 20 days for conventional aerobic treatments to 20 hours at 55ºC for advanced stabilisation treatments. However, a typical tendency in full-scale composting facilities is to shorten the composting time, basically for economic reasons. In many cases, working facilities that were designed to treat a specific amount of waste, have faced the necessity to treat a higher amount of material by using the same infrastructure, thus becoming overloaded. Therefore, in this situation, the affordable solution to reach their objectives is to decrease the composting time, but with

the downside that it can finally provoke an adverse impact on the proper biological stabilisation and/or the gaseous emission of some pollutants such as volatile organic compounds and ammonia, which are typical precursors of odour impact and annoyance.

To assess the overall treatment efficiency of a composting process, a reliable measure of the biodegradable organic matter content in organic wastes is necessary (Lasaridi and Stentiford, 1998). Numerous references can be found in literature where different methodologies are suggested as a measure of biodegradable organic matter, based on chemical or biological assays, but some of these methodologies such as the volatile solid content cannot express the potential biodegradability or stability of the waste (Ponsá et al., 2010). The methodologies based on biological assays and respiration indices are presented as more suitable tools for biodegradability and/or stability assessment. Among all available respirometric techniques, several European countries have adopted the indices proposed by the European Commission in its 2nd Draft of the Working Document on Biological Treatment of Biowaste (CIC, 2017). This regulation proposes, among other respirometric methods, the Dynamic Respirometric Index (DRI), which has been proved to be very useful for monitoring the performance of a wide variety of full-scale waste treatment facilities (Ponsá et al., 2008; Scaglia et al., 2011), for the prediction of the stability of final products such as stabilized material for landfill or compost (Barrena et al., 2014) and as a tool to monitor the performance of biological waste treatments when assessing environmental impacts of different waste treatment technologies (Colón et al., 2012). Biological stability of the material is defined as the measure of the decomposition grade of the easily biodegradable OM contained in a matrix (Lasaridi and Stentiford, 1998). The European Commission proposed in the Working Document of Biological Treatment on Biowaste, 2nd Draft (CIC, 2017), the use of the DRI –among other

parameters- to define if a material is completely stabilized or not. In the case of the DRI, a waste can be characterized as stabilized if DRI is below 1 g $O_2 \cdot kg^{-1}$ VS$\cdot h^{-1}$.

Although the main objective of sewage sludge composting is to biologically stabilize the waste and to reduce its environmental impact, its treatment and storage causes unavoidable environmental and social concerns such as gaseous emissions, which are responsible for odour nuisance. Thus, benefits of the technology can be increased or decreased depending on the associated emissions (Colón et al., 2012). Such gaseous emissions are typically generated by the decomposition of organic matter, nitrogen and sulphur-based compounds, are constituted mainly by ammonia and trace amounts of a wide range of volatile organic compounds (VOCs) (e.g., terpenes, alcohols, ketones, sulphur-containing compounds and amines), which are the main responsible for the odour nuisance (Komilis et al., 2004; Lebrero et al., 2013; Maulini-Duran et al., 2013), and are usually characterised by high flow rates and low pollutant concentrations (Colón et al., 2009). Ammonia emission, which historically has received much attention as it is the main nitrogen gas generated during composting and it can be released in huge amounts along the biological process, is related directly to the content of ammonium, urea and other organic nitrogen in the biomass and, similarly to VOCs, is dependent on temperature, aeration, pH of the composting material (Hellebrand and Kalk, 2001), as well as on biological waste reactivity (D'Imporzano et al., 2008). Ammonia is an air pollutant that contributes to eutrophication and acidification of terrestrial ecosystems. At the same time, ammonia is making an increasing relative contribution to particulate matter, with its associated human health risks. By 2020, it is estimated that NH_3 will be the largest single contributor to acidification, eutrophication and secondary particulate matter in Europe (Sutton et al., 2009). In the case of VOCs emission, depending on the quality of the treatment operation (incomplete or insufficient aeration, incomplete aerobic

5

degradation, etc.), different compounds such as intense odorous sulphur compounds, alcohols or organic acids can be released (Hommas and Fischer, 1992). Aside from being part of those main responsible of odour impact from the composting processes, VOCs in the atmosphere participate in photochemical reactions producing photochemical oxidants such as tropospheric ozone (Horowitz, 2010).

Different authors have studied gaseous emissions during sewage sludge composting in different conditions, from laboratory-scale to full-scale with different objectives. For example, Pagans et al. (2006) showed the dependency of ammonia emission on process temperature when composting different organic wastes (including sewage sludge) in a 30 L laboratory reactor, Shen et al. (2012) were able to obtain VOCs emission factors from a well-operated sewage sludge composting plant using an online monitoring method, or Awasthi et al. (2016), who studied the effect of sewage sludge co-composting with biochar and lime on the reduction of the emission of ammonia and greenhouse gases using a 130 L reactor.

The main objective of this work was to study the impact of increasing the composting process time in an industrial installation of sewage sludge composting on the waste stability and the ammonia and total volatile organic compounds (tVOCs) emissions generated along the process, focusing on both the composting phase and the curing phase. To our knowledge, this is the first study where the effect of the composting residence time over the emission factors of NH_3 and tVOCs is evaluated, providing the emission factors for a full-scale sewage sludge composting plant and allowing a comparison among similar treatment processes with different input wastes (raw sludge, municipal solid waste, etc.).

2. Material and methods

6

2.1. Composting plant

The composting plant studied is a full-scale sewage sludge composting plant located in Majorca (Spain) that treats about 8000 Mg·year^{-1} of raw sludge (RS) from primary and secondary settlers of different wastewater treatment plants. As bulking agent, 5000 Mg·year^{-1} of vegetal fraction (VF) provided by the pruning of parks and gardens is used, where two parts of fresh bulking agent and one part of reused bulking agent are mixed with RS in a 1:3 v/v ratio (1:1.2 w/w ratio) before entering the composting process. Finally, the plant produces an average of 4000 Mg·year^{-1} of compost. Table 1 shows the physicochemical properties of the two main RS treated at the composting plant, which are a mixture of primary and secondary settlers sludge provided by two different wastewater treatment plants from Majorca (RS1 and RS2, respectively), the bulking agent (VF), the initial mixture prepared in the plant (RS – VF) and the final compost obtained.

The composting process consists of two different stages, an initial high-rate decomposition stage of controlled degradation of the organic matter carried out in four dynamic windrows of approximately 30 m long, 3 m wide and 1.5 m height, followed by a curing stage of the treated material in trapezoidal piles of 170 Mg approximately. The plant's typical operation of the first stage has a windrow residence time (WRT) of 4 days (4-days WRT), working in a semi continuous way where material is loaded and unloaded daily and mixed 3 times per day with an automatic mixer, whereas the curing stage normally has a duration of 31 days, turning the material every two weeks. These normal conditions will be referred as the control experiment, which was carried out in windrows 1 and 2.

In this study, the residence time of the waste was increased from 4 to 14 days (14-days WRT) in two out of four dynamic windrows (windrows 3 and 4) by reducing the mixing ratio to 1 time every 3 days, to compare the organic matter degradation, the biological

7

stability of the product and the gaseous emission of VOCs and NH$_3$ in both scenarios. The other two dynamic windrows (windrows 1 and 2) continued working under normal conditions. The curing step time was set at 31 days for the control experiment and at 21 days for the 14-days WRT strategy due to logistic issues and spatial constraints. Figures 1S, 2S and 3S in Supplementary Information show the setup of the plant during the study, and Figure 4S in Supplementary Information shows a diagram of the whole composting process.

During the studied period, the plant treated a total of 345 Mg of the RS – VF mixture, approximately. Each windrow treated about 86 Mg of material to form two similar curing piles with 170 Mg of composted RS – VF mixture each, approximately (pile 1 referring to the curing pile formed with material treated in the 4-days WRT control process and pile 2 referring to the curing pile formed with material treated in the 14-days WRT process). For process monitoring, the material temperature and VOCs and NH$_3$ concentration in the gaseous emissions were measured two times per week during the whole study. Moisture (%), organic matter content (OM, %) and biological stability in terms of dynamic respiration index (DRI, section 2.2.2) of thirteen different samples – from the raw sludge until the final product– were determined. These thirteen samples represent different stages of the process: the raw sludge (RS1 and RS2), the mixed raw material (RS – VF), the composted RS – VF mixture (for both WRT), the initial time of the curing phase (for both piles), 17 days of curing process (for both piles), the final material before screening (for both piles) and the obtained compost once the material is sieved and refined to remove the bulking agent (for both processes) (Table 1S of Supplementary Information). As additional information, a 63% of the final material before refining is VF, which is recycled after screening.

8

The study was carried on during the months of August and September of 2016, where average temperature was 24.5ºC, average relative humidity was 66% and average wind velocity was 9.4 km·h^{-1}. The studied period was selected as it includes the weeks where more odour problems are expected to occur, given the ambient temperature.

2.2. Biological stability assessment

2.2.1. Solids sampling

During the whole study, thirteen different samples were analysed in triplicates in order to determine the moisture, the organic matter content and the biological stability of the material throughout the process (Table 1S of Supplementary Information). Because of the heterogeneity of the material, representative samples from different stages of the process were obtained by means of the quartering method (Cosenza et al., 2018). In brief, solid samples obtained from the stored raw material were taken from eight different points, which were chosen by dividing the whole material surface into eight similar sections, in order to have a representative sample of about 8 kg. Similarly, solid samples obtained from the outlet of the dynamic windrows were taken from four different points of the last two meters of the windrow, which were chosen by dividing the surface into four similar sections to have a representative sample of about 8 kg. To have a representative sample of about 8 kg, solid samples obtained from the curing piles were taken from eight different points following the same strategy as for the raw material.. Finally, all samples were frozen to -20ºC and stored until the moment of analysis, which causes no changes in their properties, as previously reported (Pognani et al., 2012).

2.2.2. Biological stability analysis

Based on the methodology proposed in different works to assess the degree of biological stability of the material (Barrena et al., 2005; Adani et al., 2006), the dynamic

respiration index (DRI) was measured using a dynamic respirometer (Ponsá et al., 2010).

The determination consists of placing 120 to 150 g of sample in a 500 mL Erlenmeyer

flask and incubating the sample in a water bath at 37 ºC. A constant airflow is supplied

through the sample, and the oxygen content in the outgoing gases is measured by means

of an oxygen sensor. From this assay, DRI was determined as the maximum average value

of respiration activity measured during 24 hours according to Eq. 1 (Ponsá et al., 2010).

$$DRI_{24h} = \frac{(O_{2,24h} - O_{2,0}) \cdot F \cdot 31.98}{22.4 \cdot 10^3 \cdot DM}$$
Eq. (1)

where DRI_{24h} is the average dynamic respiration index during the 24 hours of

maximum biological activity (g $O_2 \cdot kg^{-1}$ $DM \cdot h^{-1}$); $O_{2,24h}-O_{2,0}$ is the difference in oxygen

content between airflow in and out the reactor at 24 hours of maximum biological activity

(molar fraction); F is the volumetric airflow measured under normal conditions (1 atm

and 273 K) (mL·h^{-1}); 31.98 is the oxygen molecular weight (g·mol^{-1}); 22.4·10^3, volume

occupied by a mole of ideal gas under normal conditions (mL); DM, dry mass of the

mixture loaded in the respirometer (kg).

2.3. Determination of temperature

The material temperature was measured using a PT-100 temperature sensor installed

in a 1.5 m probe. 15 different sampling points were defined over the surface of the

material in each dynamic windrow and curing pile as shown in Figure 4S of

Supplementary Information, where the temperature of the material was measured at a 60-

80 cm depth. This methodology was used for both the dynamic windrows and the curing

piles.

2.4. Determination of gaseous emission

Total VOCs measurements were carried out using a MiniRAE 3000 PID equipped with a 9.8 eV lamp (RAE Systems MiniRAE 3000, San José, CA, USA). VOCs detection ranged from 0.1 to 15000 ppm_{veq} isobutylene (0.1 ppm_v increments). A 9.8 eV lamp was selected because the ammonia ionization energy is higher than that of the lamp photons can measure. Thus, ammonia interferences are avoided.

NH_3 concentration was measured using a manual aspiration pump (Gastec Corporation GV-100S, Ayase-Shi, Kanagawa, Japan) to pass the gas through a colorimetric tube (Gastec Corporation, Ayase-Shi, Kanagawa, Japan) with a detection range from 2.5 to 200 ppm_v of NH_3.

The emitted gas velocity was not measured during sampling period but estimated for each sampling point according to Veeken et al. (2002) and Szanto et al. (2007). A gas velocity was assumed for all the emitting surfaces of the windrows or piles (0.017 $m \cdot s^{-1}$). This velocity was corrected with a temperature factor, as shown in Eq. 2, using a reference temperature of 45 ºC and the real temperature of the material at the sampling point.

$$v_{corrected} = v_{theoretical} \cdot \frac{T_{material}}{T_{reference}}$$ Eq. (2)

where $v_{corrected}$, corrected gas velocity ($m \cdot s^{-1}$); $v_{theoretical}$, assumed gas velocity ($m \cdot s^{-1}$); $T_{material}$, temperature of the material at the sampling point (ºC); $T_{reference}$, reference temperature (45 ºC).

These gas velocities were checked in later sampling campaigns (August – September 2017), using a thermal anemometer (Testo Ltd Testo-425, Alton Hampshire, UK) with a measuring range from 0 to 20 $m \cdot s^{-1}$ and a resolution of 0.01 $m \cdot s^{-1}$ and a homemade Venturi tube, which was placed over the emitting surface to increase 22.6 times the air velocity but keeping the airflow laminar (Veeken et al., 2002; Cadena et al., 2009a). It was lately observed that differences between average estimated velocities and average

measured velocities were between 1 and 24%, being the former higher than the latter (data in Table 2S of Supplementary Information).

With the aim of determining the total pollutant load and the total emitted mass of each pollutant during the entire material processing, the methodology proposed by Cadena et al. (2009b) was used. Briefly, a matrix of sampling points covering the entire emitting surface of each windrow and curing pile is defined –as shown in Figure 4S– to determine the exhaust air velocity ($m \cdot s^{-1}$) and the pollutant concentration present in the gaseous emission ($mg \cdot m^{-3}$) in each sampling point. Then, the mass flow of each pollutant emitted per surface area unit ($mg \cdot s^{-1} \cdot m^{-2}$) is determined. Then, the emission data obtained each sampling day is represented in a three-dimension contour graph (SigmaPlot 12.0, Systat Software Inc., San Jose, CA, USA), with windrow or pile length and perimeter as x and y-axis and pollutant mass flow per surface area unit as z-axis, where each pollutant emission per area unit is presented as iso-emission curves. Multiplying the pollutant mass flow per area unit by the corresponding area in the graph in m^2 (obtained with ImageJ software, National Institutes of Health, Bethesda, MD, USA) resulted in the compound mass flow, and the sum of the different quantities obtained corresponds to the total mass flow of a pollutant ($mg \cdot s^{-1}$). Finally, each pollutant mass flow obtained for each sampling day are represented versus process time so the area below the curve obtained corresponds to the total mass of a given pollutant emitted throughout the composting process studied.

3. Results

3.1. Composting process performance

3.1.1. Temperature

During the composting and curing processes, evolution of the temperature of the material provides information about process performance, especially at full scale.

According to different authors (Stentiford et al., 1998; Li et al., 2013; Yuan et al., 2016), a maximum temperature of 65ºC is necessary to destroy pathogen microorganisms. Temperatures in the range of 45-55ºC must be maintained to attain maximum biodegradation rates. In Figure 1, temperature contours are presented in the four dynamic windrows for one sampling day once the process reached stable conditions. The *x*-axis represents the width of each windrow whereas the *y*-axis represents the length of the windrow, where 0 m is the inlet and 30 m is the outlet of each windrow.

It is worth mentioning that the raw material was stored outside the windrows with no cover, which lead to a high initial temperature in all windrows. Temperature profile differences between dynamic windrows 1 and 2 (4-days WRT) and dynamic windrows 3 and 4 (14-days WRT) were significant. In windrows 1 and 2, thermophilic conditions were reached and no decrease to mesophilic temperatures was found at the end of the process. Temperatures were above 60ºC at the end of the first phase, clearly indicating that microbial activity was considerable and that the material was not stabilized, as discussed later. In a composting process, it is important to reach thermophilic temperature to sanitize the material by destroying pathogens and weed seeds according to regulatory requirements and then proceed to achieve mesophilic temperature for further stabilization. This behaviour was observed in windrows 3 and 4, where the temperature profiles fit with standard RS composting processes (Gea et al., 2007; Maulini-Duran et al., 2013). During the first days, material reached thermophilic conditions, and then temperature gradually felt into mesophilic conditions before taking the material out of the windrows. The outlet material temperatures were between 36ºC and 40ºC, which indicated that the composting process in the dynamic windrows was nearly to be complete and that there was little biological activity present. The temperature distribution observed in windrows 3 and 4 is optimum in terms of sanitation and gaseous emission (see section

13

3.2) because thermophilic conditions are reached at the early stages of the composting process, where pathogens and weed seeds are destroyed, but it then falls down to mesophilic temperatures, where VOCs and NH_3 are emitted at low rates.

Figure 2 shows the temperature map in the curing piles for the material treated in the 4-days and 14-days WRT dynamic windrows for two different sampling dates (7 and 14 days of curing phase). The x-axis represents the width of each curing pile whereas the y-axis represents the length of each pile. As shown in Figure 2, the material of the curing pile for the 4-days WRT process (a and b) has a temperature in the thermophilic range even 14 days after setting up the pile, whereas the temperature of the material in the curing phase for the 14-days WRT process (c and d) was near to ambient in just 7 days of process. These differences indicate that the material extracted from the dynamic windrows with a WRT of 14 days is nearly stable after 7 days of curing phase. Moreover, as discussed below, the high temperatures maintained during the curing phase of the 4-days WRT process also have a direct impact on the emission of tVOCs and NH_3, increasing them in comparison to those related to the curing phase of the 14-days WRT process.

3.1.2. Biological stability

With the aim of evaluating the biological stability of the material at different times of the whole process (composting and curing), the dynamic respiration index was used.

Biological stability profiles of the material through the entire process are shown in Figure 3 as DRI of the different samples. The composted mixture corresponded to the material extracted of the dynamic windrows before being prepared for the curing phase while the final material corresponded to the compost obtained after sieving and refining the end product. The curing phase DRIs corresponded to the material at three different moments along the curing phase (0, 17 days and final material before screening).

Typical values of DRI for this kind of waste were found in both raw sludge samples (RS1 and RS2), 6.39 ± 0.96 g $O_2 \cdot kg^{-1}$ DM$\cdot h^{-1}$ and 7.27 ± 0.02 g $O_2 \cdot kg^{-1}$ DM$\cdot h^{-1}$ respectively. The fresh material, already mixed with the bulking agent, had an average DRI of 2.11 ± 0.39 g $O_2 \cdot kg^{-1}$ DM$\cdot h^{-1}$. Once the mixture passed the first treatment stage through the dynamic windrows, the DRI was reduced to 0.96 ± 0.09 g $O_2 \cdot kg^{-1}$ DM$\cdot h^{-1}$ in the 4-days WRT process and to 0.48 ± 0.15 g $O_2 \cdot kg^{-1}$ DM$\cdot h^{-1}$ in the 14-days WRT process. The higher stability achieved in the 14-days WRT process –about a 50% of DRI reduction in comparison with the 4-days WRT– has a beneficial impact on the treated material's biological stability and it also fits with typical process dynamics carried out with RS, where microorganisms have suitable conditions and enough time to degrade OM and stabilise the material (Gea et al., 2004; Ruggieri et al, 2007).

The stability of the 14-days WRT material did not change significantly from the beginning to the end of the curing process (from 0.48 ± 0.15 g $O_2 \cdot kg^{-1}$ DM$\cdot h^{-1}$ to 0.55 ± 0.01 g $O_2 \cdot kg^{-1}$ DM$\cdot h^{-1}$), whereas a DRI reduction of 57.3% (from 0.96 ± 0.09 g $O_2 \cdot kg^{-1}$ DM$\cdot h^{-1}$ to 0.41 ± 0.01 g $O_2 \cdot kg^{-1}$ DM$\cdot h^{-1}$) was obtained for the 4-days WRT material along the curing phase. In any case, considering the evolution of the biological stability along the whole process in both the 4-days and 14-days WRT scenarios, the material was stabilized indistinctly of the strategy used once the whole process was finished (composting plus curing phases). Consequently, the curing phase can be avoided increasing the WRT of the material from 4 to 14 days because the material is clearly stabilized after the composting phase.

Finally, it can be observed an increase of the DRI values from the compost samples of the 4-days WRT process and the 14-days WRT process from 0.41 to 0.83 g $O_2 \cdot kg^{-1}$ DM$\cdot h^{-1}$ and from 0.55 to 0.80 g $O_2 \cdot kg^{-1}$ DM$\cdot h^{-1}$, respectively, in comparison with the last curing phase samples. The DRI difference between the cured material (31 days) and the final

material samples can be explained according to the concentration of the OM after the sieving and refining processes to obtain the compost with the removal of the bulking agent, which is highly inert, and other non-compostable materials present in the mixture (Ruggieri et al., 2008).

3.2. Gaseous emissions

3.2.1. Dynamic windrows

Tables 2 and 3 show maximum and minimum measured concentration of each pollutant, together with the average of tVOCs and NH_3 emission rates, respectively, for the four different dynamic windrows monitored. As can be seen in Table 2, there is not a large difference between the average tVOC emission rates of each dynamic windrow, being the 14-days WRT process emission rates lightly higher. In contrast, Table 3 shows the differences in the average NH_3 emission rates between each WRT, where the 4-days WRT process emission rates are slightly higher than the 14-days WRT process emission rates. Rosenfeld et al. (2004) performed a study in which the gaseous emissions from a biosolids composting process in windrows were analysed for 13 days. During the cited study, the maximum ammonia concentration registered was about 350 ppm_v, a slightly higher value than the one measured in the present work but in a usual order of magnitude for this kind of processes.

The fact that ammonia emission rates were slightly higher in the 4-days WRT process than in the 14-days WRT process can be explained by the relation between the material temperature and the ammonia emission generated, which has been reported in previous studies (Pagans et al., 2006). When comparing the temperature maps of each windrow in Figure 1 with the emission rates presented in Table 3, it can be observed the influence of the material temperature on the emission rate of ammonia from each windrow. Generally,

16

when thermophilic conditions were reached and maintained during all the first composting phase –as in the case of windrows 1 and 2– ammonia emission rates were higher than when a typical temperature pattern was observed (first a thermophilic step followed by a mesophilic phase), as in the case of windrows 3 and 4.

Figure 4 shows an example of the emission surfaces obtained for tVOC in the dynamic windrows once stable conditions were reached. Two distributions of the tVOCs emission can be clearly distinguished between windrows 1-2 and windrows 3-4, which were similar to the temperature distributions along the windrows shown in Figure 1. When comparing the temperature distribution in Figure 1 and the emission surfaces of each windrow in Figure 4, it is observed that peaks of tVOCs emissions coincide with thermophilic phases in the dynamic windrows. However, material in windrows 1 and 2 maintain thermophilic conditions at the end of the composting phase and, in consequence, tVOCs emission do not decrease, while material in windrows 3 and 4 falls into mesophilic conditions with a concomitant decrease of the tVOCs emission. A similar behaviour can be observed in the NH_3 emissions generated in the dynamic windrows. Figure 5 shows the emission surfaces obtained once the dynamic windrows reached stable conditions. Two different distribution patterns of the ammonia emissions are observed, which are clearly related with the temperature distribution observed in the dynamic windrows. In Figures 5a and 5b, which correspond to dynamic windrows 1 and 2, ammonia emissions are distributed along the windrows, from the inlet to the outlet, being the maximum emission at the centre part of it. On the other hand, the distributions of ammonia emission observed in Figures 5c and 5d, which correspond to dynamic windrows 3 and 4, respectively, show maximum emission rates in the first days of the process –coincident with the thermophilic phase observed in Figures 1c and d–, and constantly decreases to lower values with the falling of temperature into mesophilic conditions (Pagans et al., 2006). These trends can be also

related with microbial activity present in the material, especially at the last section of the windrows, being higher the pollutant emissions generated by windrows 1 and 2 where material is not so biologically stable compared with material in windrows 3 and 4. As an additional point, Figure 5S in Supplementary Information shows the explained relationship between material's temperature and pollutant emission, using just the punctual temperature and emission values from the central sampling points of each dynamic windrows, which is analogue to what is shown in Fig. 3 and 4.

3.2.2. Curing piles

Figure 6 shows the relation between material temperature and the emission of each pollutant during the curing phase. Figure 6a shows a gradual decrease of tVOCs emission rate in pile 1 –prepared with material previously treated at the 4-days WRT windrows–, which fits with the decrease of the material temperature and biological activity during the curing phases. The emission remained high –between 0.8 and 1.1 kg C-VOC·d^{-1}– coinciding with the time that the pile temperature was over 50ºC. Maximum tVOCs concentration measured in pile 1 was 10.0 ppm_v during the first week of the curing process, when material was at thermophilic conditions. Then, emissions decrease to emission rates close to 0 kg C-VOC·d^{-1} when the process reaches mesophilic conditions, which correspond to minimum tVOCs concentration between 0.0 and 0.9 ppm_v. Different behaviours have been reported in the literature concerning tVOCs concentration in the gaseous emission when composting RS in different conditions, always at pilot-scale. Zigmontiene and Zuokaite (2010) reported maximum tVOCs concentrations around 11 ppm_v at the first days of a RS composting process. However, other authors observed higher tVOCs concentration in the gaseous emissions when composting RS mixed with different bulking agents at different mixing ratios (Pagans et al., 2005; Zuokaite and Zigmontiene, 2012), but in general the higher tVOCs concentrations appear when process

is at thermophilic conditions. On the other hand, tVOC concentrations in the emissions from pile 2 –prepared with material previously treated at the 14-days WRT windrows– were always below the lower detection limit of the VOCs sensor (0.1 ppm$_v$), which were in close agreement with the low DRI results and the mesophilic temperatures of the pile (always below 40ºC) during the whole curing process, indicating that material was already stabilized.

A similar trend was observed with ammonia emissions in both curing piles. Figure 6b shows the profiles obtained when NH$_3$ emission rate and material's average temperature values are represented versus curing process time. Among other parameters not discussed in this work, there it can be observed the close relation and dependency between material's temperature and ammonia emission rate during the curing phase of both piles 1 and 2. Moreover, this temperature-ammonia emission relation is inherent to the biological stability of the material in each pile, where curing pile 2, which had a lower DRI value, showed lower ammonia emission rates than curing pile 1. During the curing phase, maximum and minimum ammonia concentrations registered in the gaseous emissions from pile 1 were about 150 ppm$_v$ and 10 ppm$_v$, respectively. Comparing to what has been observed in other RS composting studies (Rosenfeld et al., 2004; Pagans et al., 2006), similar maximum concentrations were found when material temperature was nearly 60ºC, whereas similar minimum concentrations were measured when material temperature dropped to mesophilic conditions. On the other hand, for the curing phase of pile 2 –which was always in mesophilic conditions– the maximum and minimum values registered in the gaseous emissions were 20 ppm$_v$ and 0.5 ppm$_v$, respectively, which are lower than what has been found in similar works (Rosenfeld et al., 2004; Chen and Xin-Wu, 2010). There is a great difference between the emission rates observed in piles 1 and 2, indicating that ammonia emission is dependent on material's temperature, what fits

19

with what is mentioned in other studies (Pagans et al., 2006; Maulini-Duran et al., 2013; Yuan et al., 2015). These authors also observed that at higher process temperature, the emission of ammonia is increased and vice versa.

In general, the combination of higher temperature and higher pollutant concentration measured in pile 1 may lead to punctual environmental impacts coinciding with the moment of the turning of the pile's material, releasing a higher amount of ammonia and tVOCs in respect to what may happen with pile 2 turning.

In Figure 7, direct correlations of each pollutant emission rate with the process temperature are presented. Figure 7a shows the relation between the material temperature and tVOCs emission for both piles 1 and 2. Even though there is not a clear correlation between the data presented, the trend followed by the emission of tVOCs at the curing piles depending on the process temperature shows that when temperature is increased – reaching thermophilic conditions–, the emission of tVOCs also increases. Otherwise, when temperature is in a mesophilic range, tVOC emission is close to 0. Similarly, Figure 7b shows that the highest NH_3 emission appeared with thermophilic temperatures. The trends of ammonia emission observed in piles 1 and 2 show that the ammonia emissions generated by the RS composting increase exponentially during the thermophilic phase of the process, followed by a steady linear emission pattern at the end of the process when mesophilic conditions are reached. This relationship between process temperature and pollutant emission has been previously showed in some pilot-scale studies (Pagans et al., 2006), but this is the first time it has been observed for both tVOCs and NH_3 in a full-scale sewage sludge composting plant.

3.2.3. Emission factors

With the aim of assessing the difference of tVOC and NH_3 emitted between both processes and obtaining comparable values, an emission factor for each pollutant was calculated for each process in terms of total amount of pollutant emitted per unit of total mass to be treated per time unit, due to the semi continuous nature of the first stage of the treatment process. These results are presented in Table 4 together with the total process time for both pollutants. The emission factors for each process were calculated by relating the total amount of pollutant emitted with the total mass of RS – VF mixture treated per time unit. It is observed that the 14-days WRT process contributes in a not significant increase of the 7.7% of the C-VOC emission factor. Nonetheless, the proposed strategy contributes in a total reduction of a 32.2% of the ammonia emission factor. On the other hand, this emission data can be also presented as emission masses in terms of total mass of emitted pollutant per unit of total mass to be treated. Table 5 shows the results obtained, where an increase of both tVOCs and NH_3 emission masses is observed when increasing the WRT from 4 to 14 days. These increment in the emission masses when changing the WRT from 4 to 14 days can be explained by the fact that a similar mass is being treated during more time, so the total pollutant mass emitted will be inevitably higher.

There are some works on the emission factors obtained for sewage sludge composting experiments at pilot-scale (Maulini-Duran et al., 2013; Yuan et al., 2016), but there is lack of information in this field when reporting emission factors from full-scale sewage sludge composting facilities. However, Shen et al. (2012) could measure the total amount of tVOCs emitted in a RS composting plant per mass unit of total mixed material to be treated (raw sludge, mature compost and wood chips) and per time unit, reporting an average emission factor of 7.99 g tVOCs·Mg^{-1}total waste mixture·d^{-1}, a lower value than the one that has been obtained in the present work. Shen et al. (2012) also reported the tVOCs emission mass for the entire composting process, being 0.16 kg tVOCs·Mg^{-1}total

21

waste mixture. In pilot-scale, different emission factors and emission masses have been reported for tVOCs and NH_3 depending on the process conditions (aerated or non-aerated, RS:bulking agent ratio, etc.), ranging from 7 to 10 g tVOCs·Mg^{-1}total waste mixture·d^{-1} and from 14 to 130 g NH_3·Mg^{-1}total waste mixture·d^{-1}, or from 0.14 to 0.21 kg tVOCs·Mg^{-1}total waste mixture and from 0.28 to 1.40 kg NH_3·Mg^{-1}total waste mixture.

In conclusion, the methodology used to estimate the emission factor of different pollutants from a RS composting process in a full-scale facility is correct and reproducible, and can be a useful tool to compare tVOCs and NH_3 emissions generated by this kind of RS composting process in future studies.

4. Conclusions

A technical assessment of the influence of the composting time on the composting process performance of a full-scale sewage sludge composting plant has been done in order to categorize the waste stabilization reached and the gaseous emissions related to each kind of treatment strategy. By increasing the residence time of the material in the dynamic windrows from 4 to 14 days, the composting process experiments a more optimum evolution in terms of temperature evolution and biodegradation level achieved at the end of the first phase, what could lead to a reduction of the curing phase time in order to process more material in the same time.

A strong relation between tVOC and NH_3 emissions and material temperature was observed. Generally, higher pollutant emissions were measured when material temperature was in a thermophilic range, which also coincides with the observed material's higher biological activity. Therefore, these emissions decreased when material temperature fell into mesophilic range. Nevertheless, emission masses obtained increased

when changing the WRT from 4 to 14 days, mostly in the dynamic windrows, due to the fact that similar quantities of material are treated in a longer process.

In conclusion, when comparing both treatment strategies carried out in this particular full-scale composting facility, it is preferable to maintain a larger composting time (14-d WRT strategy) in order to achieve a proper biological stabilisation of the sewage sludge. Moreover, in terms of pollutant's impact, the emission factor of ammonia, which is one the typical odour nuisance precursors of this kind of biological processes, is decreased and that would help to mitigate punctual odour impacts generated by the plant. Although the mentioned benefits, this working strategy could compromise the economical balance of the composting plant for two reasons: first of all, if working with the same infrastructure, its treatment capacity (Mg of RS·year^{-1}) would be reduced, so less waste would be treated every year; on the other hand, if it is desired to maintain or even increase the plant treatment capacity, an investment in reshape and enlargement of the infrastructure should be done.

Although environmental and economical assessment of each treatment strategy could be the object for further studies and discussion, this study sets a comparison of different operation strategies in terms of waste stabilisation and gaseous emissions, which results can be helpful for plant managers and operators in order to choose different operation strategies when treating sewage sludge.

23

References

Adani, F., Ubbiali, P., Genevini, P., 2006. The determination of biological stability of composts using the dynamic respiration index: the results of experience after two years. Waste Management. 26, 41-48.

Awasthi, M. K., Wang, Q., Huang, H., Li, R., Shen, F., Lahori, A. H., Wang, P., Guo, D., Guo, Z., Jiang, S., Zhang, Z., 2016. Effect of biochar amendment on greenhouse gas emission and bio-availability of heavy metals during sewage sludge co-composting. Journal of Cleaner Production. 135, 829-835.

Barrena, R., Vázquez, F., Gordillo, M. A., Gea, T., Sánchez, A., 2005. Respirometric assays at fixed and process temperatures to monitor composting process. Bioresource Technology. 96, 1153-1159.

Barrena, R., Font, X., Gabarrell, X., Sánchez, A., 2014. Home composting versus industrial composting: Influence of composting system on compost quality with focus on compost stability. Waste Management. 34, 1109-1116.

Cadena, E., Colón, J., Artola, A., Sánchez, A., Font, X., 2009a. Environmental impact of two aerobic composting technologies using life cycle assessment. International Journal of Life Cycle Assessment. 14, 401-410.

Cadena, E., Colón, J., Sánchez, A., Font, X., Artola, A., 2009b. A methodology to determine gaseous emissions in a composting plant. Waste Management. 29, 2799-2807.

Chen, L., Xin-Wu, W., 2010. Reduction of ammonia, hydrogen sulphide and short-chain fatty acids emission during the sewage sludge composting. Clean – Soil, Air, Water. 38 (11), 998-1005.

CIC, 2017. Consorzio Italiano Compostatori. Working document of biological treatment on biowaste, 2nd Draft (European Commission). http://www.compost.it/www/pubblicazioni_on_line/biod.pdf , Accessed on September 2017.

Colón, J., Martínez-Blanco, J., Gabarrell, X., Rieradevall, J., Font, X., Artola, A., Sánchez, A., 2009. Performance of an industrial biofilter from a composting plant in removal of ammonia and VOCs after material replacement. Journal of Chemical Technology and Biotechnology. 84(8), 1111-1117.

Colón, J., Cadena, E., Pognani, M., Barrena, R., Sánchez, A., Font, X., Artola, A., 2012. Determination of the energy and environmental burdens associated with the biological treatment of source-separated municipal solid wastes. Energy and Environmental Science. 5, 5731-5741.

Colón, J., Alarcón, M., Healy, M., Namli, A., Ponsá, S., Sanin, F. D., Taya, C., 2017. Producing sludge for agricultural applications. In: Innovative wastewater treatment and resource recovery technologies (J. M. Lema & S. Suárez Martínez Eds.). IWA Publishing, London.

Cosenza, A., Di Bella, G., Torregrossa, M., Viviani, G., 2018. Biological stability of organic fraction of municipal solid wastes during composting processes. Environmental Engineering Science. 32 (1).

D'Imporzano, G., Crivelli, F., Adani, F., 2008. Biological compost stability influences odor molecules production measured by electronic nose during food-waste high-rate composting. Science of the Total Environment. 402, 278-284.

European Commission, 2010. Working document of sludge and biowaste. Directorate General Environment. Brussels.

Eurostat, 2015. Sewage sludge production and disposal database 2004-2015. European Commission. http://ec.europa.eu/eurostat/tgm/table.do?tab=table&plugin=1&language=en&pcode=ten00030 , Accessed on November 2017.

Gea, T., Barrena, R., Artola, A., Sánchez, A., 2004. Monitoring the biological activity of the composting process: oxygen uptake rate (OUR), respirometric index (RI) and respiratory quotient (RQ). Biotechnology and Bioengineering. 88, 417-546.

Gea, T., Barrena, R., Artola, A., Sánchez, A., 2007. Optimal bulking agent particle size and usage for heat retention and disinfection in domestic wastewater sludge composting. Waste Management. 27, 1108-1116.

Hellebrand, H. J., Kalk, W. D., 2001. Emission of methane, nitrous oxide and ammonia from dung windrows. Nutrient Cycling Agroecosystems. 60, 83-87.

Hommas, W. J., Fischer, K., 1992. A composting plant as an odour source, compost as an odour killer. Acta Hortic. 302, 37-44.

Horowitz, R., 2010. Are compost emissions a strong ozone source? BioCyle. 51(3), 18-22.

Komilis, D. P., Ham, R. K., Park, J. K., 2004. Emissions of volatile organic compounds during composting of municipal solid wastes. Water Research. 38, 1707-1714.

Kosobucki, P., Chmarzyński, A., 2000. Sewage sludge composting. Polish Journal of Environmental Studies. 9, 243-248.

Lasaridi, K. E., Stentiford, E. I., 1998. A simple respirometric technique for assessing compost stability. Water Research. 38, 1708-1714.

Lebrero, R., Rangel, M. G. L., Muñoz, R., 2013. Characterization and biofiltration of a real odorous emission from wastewater treatment plant sludge. Journal of Environmental Management. 116, 50-57.

Li. Z., Lu., H., Ren, L., He, L., 2013. Experimental and modeling approaches for food waste composting: A review. Chemosphere. 93, 1247-1257.

Maulini-Duran, C., Artola, A., Font, X., Sánchez, A., 2013. A systematic study of the gaseous emissions from biosolids composting: Raw sludge versus anaerobically digested sludge. Bioresource Technology. 147, 43-51.

Pagans, E., Font, X., Sánchez, A., 2005. Emission of volatile organic compounds from composting of different solid wastes : Abatement by biofiltration. Journal of Hazardous Materials. B131, 179-186.

Pagans, E., Barrena, R., Font, X., Sánchez, A., 2006. Ammonia emissions from the composting of different organic wastes. Dependency on process temperature. Chemosphere. 62, 1534-1542.

Pognani, M., Barrena, R., Font, X., Sánchez, A., 2012. Effect of freezing on the conservation of the biological activity of organic solid wastes. Bioresource Technology. 104, 832-836.

Ponsá, S., Gea, T., Alerm, L., Cerezo, J., Sánchez, A., 2008. Comparison of aerobic and anaerobic stability indices through a MSW biological treatment process. Waste Management. 28, 2735-2742.

Ponsá, S., Gea, T., Sánchez, T., 2010. Different indices to express biodegradability in organic solid wastes. Journal of Environmental Quality. 39, 706-712.

Rosenfeld, P., Grey, M., Sellew, P., 2004. Measurement of biosolids compost odor emissions from a windrow, static pile and biofilter. Water Environment Research. 76 (4), 310-315.

Ruggieri, L., Gea, T., Artola, A., Sánchez, A., 2007. Influence of different co-substrates biochemical composition on raw sludge co-composting. Biodegradation. 19, 403-415.

Ruggieri, L., Gea, T., Mompeó, M., Sayara, T., Sánchez, A., 2008. Performance of different systems for the composting of the source-selected organic fraction of municipal solid waste. Biosystems Engineering. 101, 78-86.

Sadef, Y., Poulsen, T. G., Bester, K., 2014. Impact of compost process temperature on organic micro-pollutant degradation. Science of the Total Environment. 494-495, 306-312.

Sánchez, A., Gabarrell, X., Artola, A., Barrerna, R., Colón, J., Font, X., Komilis, D., 2015. Composting of wastes. In: Resource recovery to approach zero municipal waste. Green Chemistry and Chemical Engineering Series (Taherzadeh, M. J., Richards, T., Eds.), pp 77-106. CRC Press, Taylor & Francis Group.

Scaglia, B., Orzi, V., Artola, A., Font, X., Davoli, E., Sánchez, A., Adani, F., 2011. Odours and volatile organic compounds emitted from municipal solid waste at different stage of decomposition and relationship with biological stability. Bioresource Technology. 102, 4638-4645.

Shen, Y., Chen, T. B., Gao, D., Zheng, G, Liu, H., Yang, Q., 2012. Online monitoring of volatile organic compound production and emission during sewage sludge composting. Bioresource Technology. 123, 463-470.

Stentiford, E., Mara, D., Taylor, P. L., 1998. Forced aeration co-composting of domestic refuse and sewage sludge in static piles. In: Composting of Agricultural and other Wastes (Gasser J KR, Ed), pp 42-55. Elsevier Applied Science Publishers, London.

Sutton, M.A., Reis, S., Baker, S., 2009. Atmospheric ammonia, detecting emission changes and environmental impacts – Results of an Expert Workshop under the Convention on Long-range Transboundary Air Pollution. Springer Science.

Szanto, G. L., Hamelers, H. V. M., Rulkens, W. H., Veeken, A. H. M., 2007. NH3, N2O and CH4 emissions during passively aerated composting of straw-rich pig manure. Bioresource Technology. 98, 2659-2670.

Veeken, A., de Wilde, V., Hamelers, B., 2002. Passively aerated composting of straw-rich pig manure: Effect of compost bed porosity. Compost Science & Utilization. 10 (2), 114-128.

Yuan, J., Chadwick, D., Zhang, D., Li, G., Chen, S., Luo, W., Du, L., He, S., Peng, S., 2016. Effects of aeration rate on maturity and gaseous emissions during sewage sludge composting. Waste Management. 56, 403-410.

Zigmontiene, A., Zuokaite, E., 2010. Investigation into emissions of gaseous pollutants during sewage sludge composting with wood waste. Journal of Environmental Engineering and Landscape Management. 18 (2), 128-136.

Zuokaite, E., Zigmontiene, A., 2012. Application of natural cover during sewage sludge composting to reduce gaseous emissions. Polish Journal of Environmental Studies. 22 (2), 621-626.

Legends to Figures

Figure 1. Temperature map of each dynamic windrow, in ºC (a) dynamic windrow 1, 4-days WRT, (b) dynamic windrow 2, 4-days WRT, (c) dynamic windrow 3, 14-days WRT, (d) dynamic windrow 4, 14-days WRT.

Figure 2. Temperature maps of the curing piles, in ºC (a) 7 days of curing of a material with 4-days WRT, (b) 14 days of curing of a material with 4-days WRT, (c) 7 days of curing of a material with 14-days WRT, (d) 14 days of curing of a material with 14-days WRT.

Figure 3. Biological stability of the material at different moments of it processing, expressed by DRI values (grey bars: RS1, RS2 and RS – VF mixture; black bars: process with a material WRT of 4 days in the dynamic windrows; white bars: process with a material WRT of 14 days in the dynamic windrows; error bars of the values obtained in three replicates).

Figure 4. tVOCs iso-emission curves of the dynamic windrows studied for a sampling date, in mg of C-VOC$\cdot$m$^{-2}\cdot$s^{-1} (a) dynamic windrow 1, 4-days WRT, (b) dynamic windrow 2, 4-days WRT, (c) dynamic windrow 3, 14-days WRT, (d) dynamic windrow 4, 14-days WRT.

Figure 5. NH_3 iso-emission curves of the dynamic windrows studied for a sampling date, in mg of $NH_3\cdot$m$^{-2}\cdot$s^{-1} (a) dynamic windrow 1, 4-days WRT, (b) dynamic windrow 2, 4-days WRT, (c) dynamic windrow 3, 14-days WRT, (d) dynamic windrow 4, 14-days WRT.

Figure 6. (a) tVOCs emission rate and material temperature during the curing phase of both curing piles studied (black dots: tVOCs emission rates of pile 1; white dots: average temperature in pile 1; black diamonds: tVOCs emission rates of pile 2; white diamonds: average temperature in pile 2). (b) NH_3 emission rate and material temperature during the curing phase of both curing piles studied (black dots: NH_3 emission rates of pile 1; white dots: average temperature in pile 1; black diamonds: NH_3 emission rates of pile 2; white diamonds: average temperature in pile 2).

Figure 7. (a) Correlation of tVOCs emission vs. temperature for curing piles 1 and 2 (black dots: tVOCs emission rates of pile 1; black diamonds: tVOCs emission rates of pile 2). (b) Correlation

of NH_3 emission vs. temperature for curing piles 1 and 2 (black dots: NH_3 emission rates of pile 1; black diamonds: NH_3 emission rates of pile 2).

Tables

Table 1. Physicochemical properties of the two main raw sludge treated at the plant (RS1 and RS2), the bulking agent (VF), the RS – VF mixture and the final compost.

Physicochemical properties	RS1	RS2	VF	RS – VF mixture	Compost
Moisture (%)	86.8 ± 0.0	86.1 ± 0.0	15.5 ± 0.4	58.3 ± 0.5	46.0 ± 0.2
Organic matter (%)	79.1 ± 0.2	84.4 ± 0.5	85.3 ± 2.1	79.1 ± 1.2	64.2 ± 1.6
C/N ratio	7.0	6.5	50.0	28.9	21.4
pH	6.57	6.79	8.41	7.16	–
Electrical conductivity (mS/cm)	2.41	2.38	0.95	2.91	–
Dynamic Respiration Index ($g\ O_2 \cdot kg^{-1}\ DM \cdot h^{-1}$)	6.39 ± 0.96	7.27 ± 0.02	–	2.11 ± 0.23	0.83 ± 0.07

Table 2. tVOCs emission rates and maximum and minimum concentrations (in ppm_v) from the four dynamic windrows studied.

Time (d)	tVOC emission rate windrow 1 (kg C-VOC·d^{-1})	tVOC concentration (ppm_v) MAX	MIN	tVOC emission rate windrow 2 (kg C-VOC·d^{-1})	tVOC concentration (ppm_v) MAX	MIN	tVOC emission rate windrow 3 (kg C-VOC·d^{-1})	tVOC concentration (ppm_v) MAX	MIN	tVOC emission rate windrow 4 (kg C-VOC·d^{-1})	tVOC concentration (ppm_v) MAX	MIN
0	2.111	15.1	2.4	2.282	14.1	1.6	2.761	14.8	6.0	2.601	15.1	8.0
4	1.799	9.8	2.8	1.495	8.3	2.4	2.238	14.5	3.0	2.558	15.2	4.0
10	-	-	-	-	-	-	2.822	16.6	2.8	2.156	16.8	2.5
14	-	-	-	-	-	-	3.082	16.8	1.1	2.658	18.0	1.8

Table 3. NH_3 emission rates and maximum and minimum concentrations (in ppm_v) from the four dynamic windrows studied.

Time (d)	NH_3 emission rate windrow1 (kg $NH_3 \cdot d^{-1}$)	NH_3 concentration (ppm_v)		NH_3 emission rate windrow2 (kg $NH_3 \cdot d^{-1}$)	NH_3 concentration (ppm_v)		NH_3 emission rate windrow3 (kg $NH_3 \cdot d^{-1}$)	NH_3 concentration (ppm_v)		NH_3 emission rate windrow4 (kg $NH_3 \cdot d^{-1}$)	NH_3 concentration (ppm_v)	
		MAX	MIN		MAX	MIN		MAX	MIN		MAX	MIN
0	12.437	200	80	10.859	180	100	8.458	120	100	11.252	160	120
4	13.205	180	120	12.159	160	80	9.312	140	100	10.862	140	120
10	-	-	-	-	-	-	12.434	220	60	8.571	220	60
14	-	-	-	-	-	-	12.002	250	30	9.665	250	50

Table 4. Individual (windrow and curing phase) and global C-VOC and NH$_3$ emission factors for each type of composting process studied.

Pollutant	Process	Total time	Windrow phase emission factor (g pollutant·Mg^{-1} RS – VF·d^{-1})	Curing phase emission factor (g pollutant·Mg^{-1} RS – VF·d^{-1})	Global emission factor (g pollutant·Mg^{-1} RS – VF·d^{-1})
C-VOC	4-days WRT	4 days in dynamic windrow + 31 days of curing	23.7	2.3	26.0
	14-days WRT	14 days in dynamic windrows + 21 days of curing	28.0	0.0	28.0
NH3	4-days WRT	4 days in dynamic windrow + 31 days of curing	150.0	26.0	176.0

	14 days in dynamic			
14-days WRT	windrows + 21 days	113.2	1.1	114.3
	of curing			

Table 5. Emission mass of tVOCs and NH_3 for each type of composting process studied.

Process	Total time	Windrow phase emission mass		Curing phase emission mass		Global emission mass	
		C-VOC (kg C-VOC·Mg^{-1} RS – VF)	NH_3 (kg NH_3·Mg^{-1} RS – VF)	C-VOC (kg C-VOC·Mg^{-1} RS – VF)	NH_3 (kg NH_3·Mg^{-1} RS – VF)	C-VOC (kg C-VOC·Mg^{-1} RS – VF)	NH_3 (kg NH_3·Mg^{-1} RS – VF)
4-days WRT	4 days in dynamic windrows + 31 days of curing	0.09	0.60	0.07	0.61	0.16	1.21
14-days WRT	14 days in dynamic windrows + 21 days of curing	0.39	1.58	0.00	0.02	0.39	1.60

Highlights

- Composting time in a full-scale sewage sludge treatment plant was studied.

- A better process performance is achieved by increasing the composting time.

- Ammonia and VOCs emission factors are presented for different strategies.

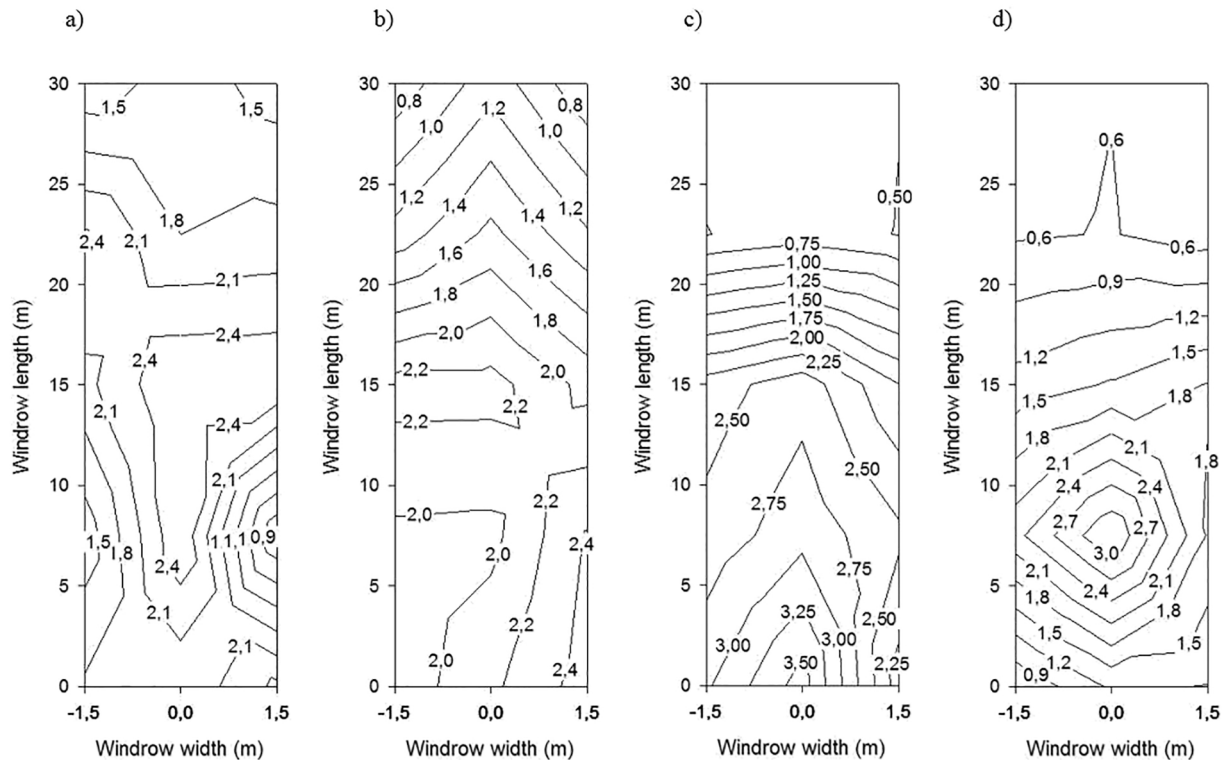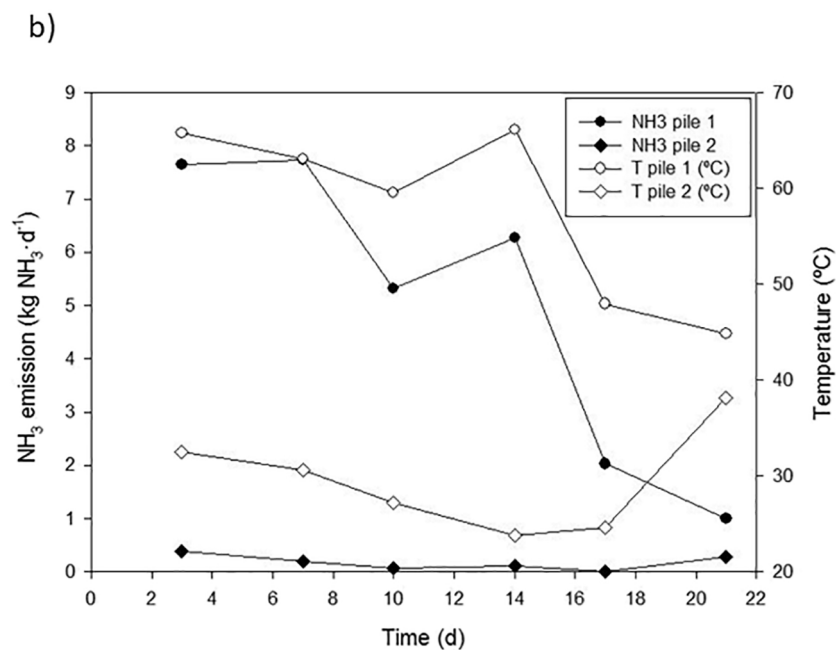- The emission factors presented are useful tools to compare treatment processes.
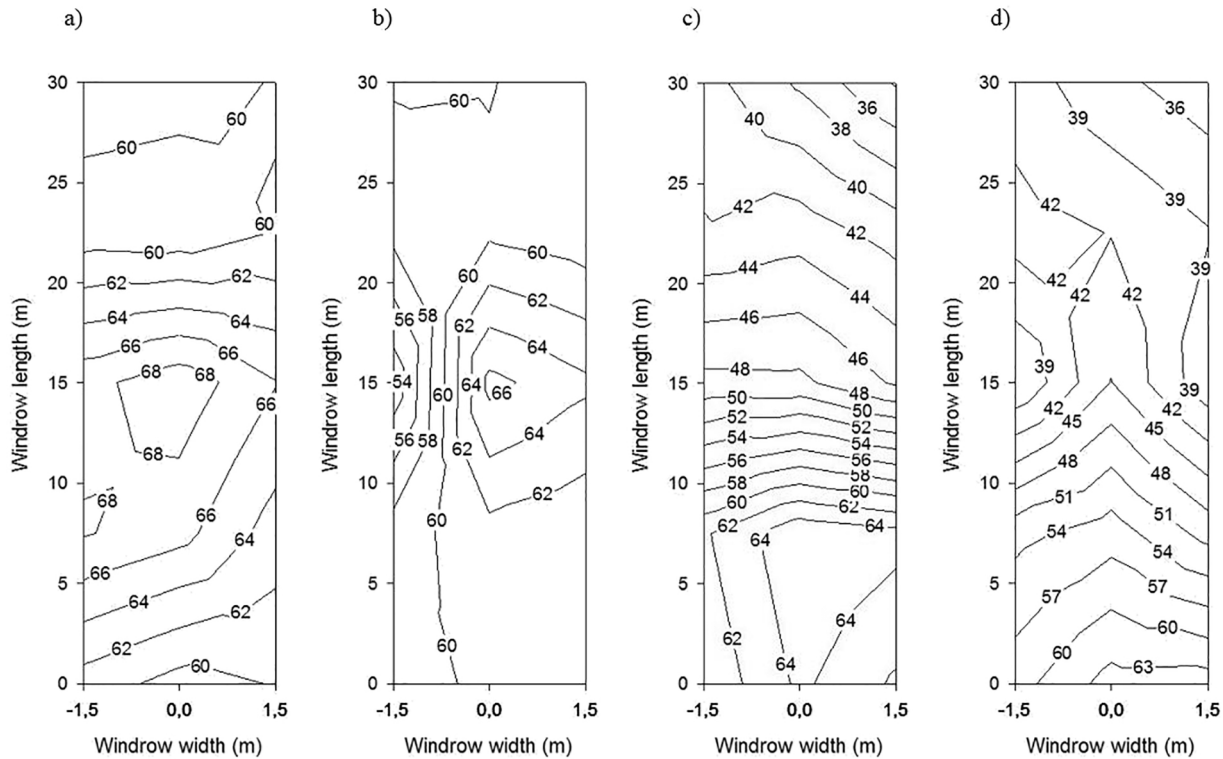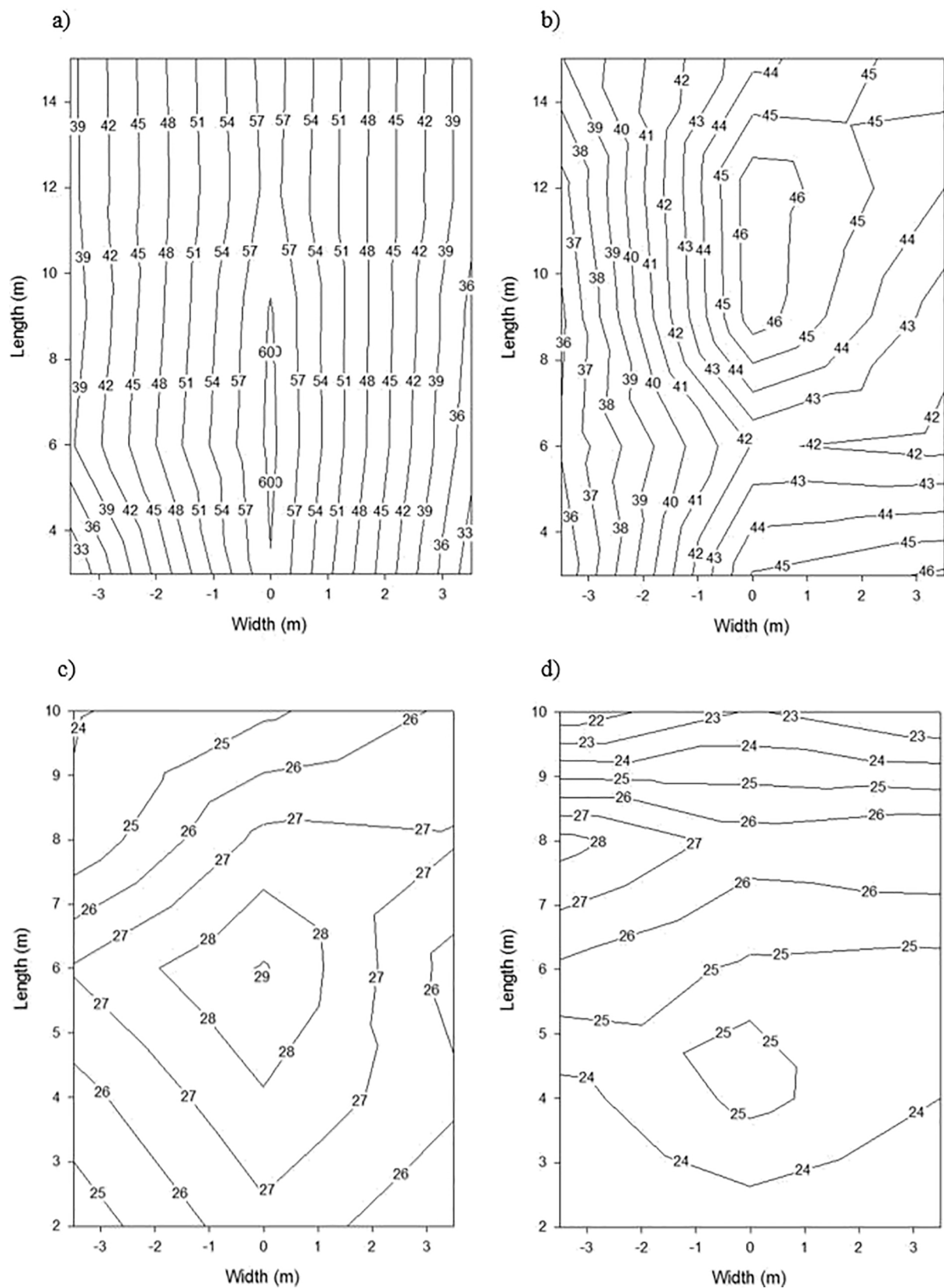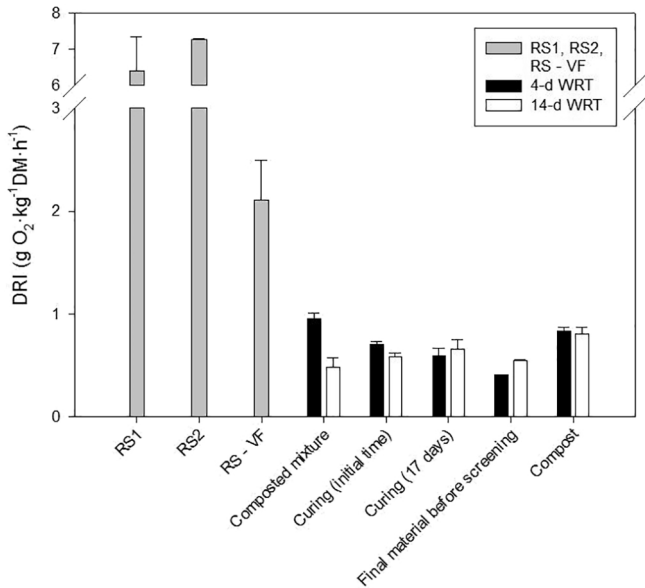
Figure 1

Figure 2

Figure 3

Figure 4

Figure 5

a)

b)

Figure 6

a)

b)

Figure 7